Available online at www.sciencedirect.com
ScienceDirect
Bioorganic & Medicinal Chemistry 15 (2007) 6596–6607
Bioorganic & Medicinal Chemistry

Synthesis, in vitro assay, and molecular modeling of new piperidine derivatives having dual inhibitory potency against acetylcholinesterase and $A\beta_{1-42}$ aggregation for Alzheimer's disease therapeutics

Young Ee Kwon,[a,*,†] Jung Youl Park,[b,†] Kyung Tai No,[c,d] Jae Hong Shin,[d] Sung Kwang Lee,[d] Jae Soon Eun,[a] Jae Heon Yang,[a] Tae Yong Shin,[a] Dae Keun Kim,[a] Byung Sook Chae,[a] Jae-Yoon Leem[a] and Kuk Hwan Kim[e]

[a]*College of Pharmacy, Woosuk University, Jeonbuk, Republic of Korea*
[b]*C&C Research Laboratories, Kyung Gi, Republic of Korea*
[c]*Department of Biotechnology, Yonsei University, Seoul, Republic of Korea*
[d]*Bioinformatics & Molecular Design Research Center, Seoul, Republic of Korea*
[e]*K&C Medicine Research Center, Bucheon, Republic of Korea*

Received 10 May 2007; revised 30 June 2007; accepted 6 July 2007
Available online 25 July 2007

Abstract—With the goal of developing Alzheimer's disease therapeutics, we have designed and synthesized new piperidine derivatives having dual action of acetylcholinesterase (AChE) and beta-amyloid peptide (Aβ) aggregation inhibition. For binding with the catalytic site of AChE, an ester with aromatic group was designed, and for the peripheral site, another aromatic group was considered. And for intercalating amyloid-beta oligomerization, long and linear conformation with a lipophilic group was considered. The synthetic methods employed for the structure with dual action depended on alcohols with an aromatic ring and the substituted benzoic acids, which are esterificated in the last step of the synthetic pathway. We screened these new derivatives through inhibition tests of acetylcholinesterase, butyrylcholinesterase (BChE), and $A\beta_{1-42}$ peptide aggregation, AChE-induced $A\beta_{1-42}$ aggregation. Our results displayed that compound **12** showed the best inhibitory potency and selectivity of AChE, and **29** showed the highest selectivity of BChE inhibition. Compounds **15** and **12** had inhibitory activities against $A\beta_{1-42}$ aggregation and AChE-induced Aβ aggregation. In the docking model, we confirmed that 4-chlorobenzene of **12** plays the parallel π–π stacking against the indole ring of Trp84 in the bottom gorge of AChE. Because the benzyhydryl moiety of **12** covered the peripheral site of AChE in a funnel-like shape, **12** showed good inhibitory potency against AChE and could inhibit AChE-induced $A\beta_{1-42}$ peptide aggregation.

1. Introduction

Alzheimer's disease (AD), the most common dementia in elderly people, is a complex neurodegenerative disorder of central nervous system. It is associated with a selective loss of cholinergic neurons and reduced levels of acetylcholine neurotransmitter. A wide range of evidence shows that acetylcholinesterase (AChE) inhibitors can interfere with the progression of AD.[1–3] The more basic pathological abnormalities in AD are amyloid plaques, neurofibrillary tangles, and neuronal death.[4,5] In the past two decades, many efforts have been made to understand the molecular pathogenesis of AD, and to carry out its early diagnosis and therapeutic control. Most relevant pathogenic events in AD can be classified into the following four categories, (1) genetic alteration, (2) beta-amyloid (Aβ) deposition in senile plaques, (3) neuroimmune dysfunction, and (4) cerebrovascular dysfunction.[4–6] All of these pathogenic events are potential targets for AD therapy, but the cholinergic neurotransmission and beta-amyloid peptide are regarded as main targets for more effective treatment strategies. The cholinergic hypothesis is still the most successful approach

Keywords: Piperidine derivatives; Alzheimer's disease; Acetylcholinesterase; Butyrylcholinesterase; $A\beta_{1-42}$ aggregation; Dual action.
* Corresponding author. Tel.: +82 63 290 1566/+82 17 257 1006; fax: +82 63 290 1812; e-mail: yekwon@woosuk.ac.kr
† These authors contributed equally to this work.

0968-0896/$ - see front matter © 2007 Elsevier Ltd. All rights reserved.
doi:10.1016/j.bmc.2007.07.003

for the symptomatic treatment of AD. This hypothesis postulates that at least some of the cognitive decline experienced by AD patients results from a deficiency in acetylcholine and thus in cholinergic neurotransmission. Therefore, inhibition of AChE appears to be a natural therapeutic strategy to palliate the cognitive deficit in AD. Thus, the AChE inhibitors such as tacrine,[7] donepezil,[8] rivastigmine[9], and galantamine[10] have been launched on the market for the symptomatic treatment of AD (Fig. 1).

Beta-amyloid peptide is a main component of the senile plaques and fibrillary tangles that constitute one of the neurohistopathological features of AD. An overproduction of Aβ peptide and its subsequent deposition as insoluble amyloid plaques may represent the key pathological pathway.[11] Accordingly, Aβ peptide has become a primary target in the development of effective therapies.[6,11] Amyloid targeted therapeutic approaches aimed at blocking the neurotoxic activity of Aβ are presently pursued for the inhibition of amyloid production by inhibiting the enzyme cleaving beta-amyloid protein precursor, immunizing against AD, and inhibition of amyloid polymerization.[12] An attractive therapeutic strategy is to inhibit peptide aggregation itself, because this appears to be the first step in the pathogenic process of amyloidosis, which is not associated with natural biological function.[13] Figure 2 shows examples of some small molecule Aβ inhibitors. Current NMR and molecular modeling studies are being conducted to unravel the structure and dynamics of Aβ peptide and to understand the molecular basis of the amyloid fibril formation.[14–17] But the lack of structural similarity among the Aβ inhibitors is striking, suggesting that they bind to different sites within amyloid in contrast to most drugs. This interferes in making conclusions from rational structure–activity relationships. Recent studies have identified that AChE enhances the aggregation of Aβ peptide fragments[18] and accelerates the assembly of $A\beta_{1-42}$ peptide into the amyloid fibrils that form the senile plaques characteristic of AD. These results, together with binding assays, have suggested that AChE may contribute to the generation of amyloid deposits and/or physically affects fibril assembly. Moreover, it has also been shown that the neurotoxicity of $A\beta_{1-42}$ peptide aggregates depends on the amount of AChE bound to the complexes, suggesting that AChE may play a key role in the neurodegeneration observed in an AD patient's brain.[19,20]

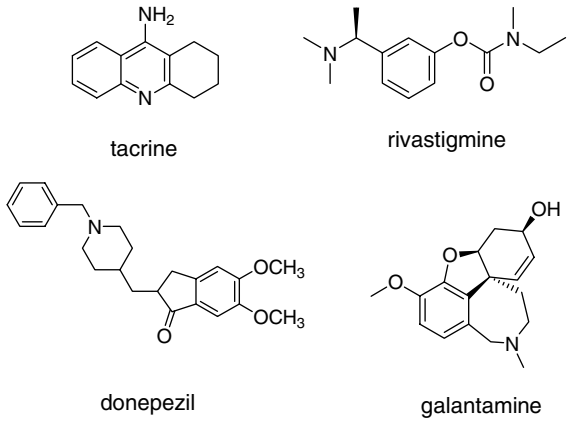

Figure 1. Structures of the acetylcholinesterase inhibitors as FDA approved Alzheimer's disease therapeutics.

We designed and synthesized new compounds with dual action of effective anti-acetylcholinesterase and $A\beta_{1-42}$ peptide aggregation inhibition. Specifically, we focused our efforts on piperidine derivatives binding with a catalytic and a peripheral site of AChE, and having inhibitory potency against Aβ aggregation. We report here the synthesis, pharmacological evaluation, and molecular modeling of new piperidine compounds.

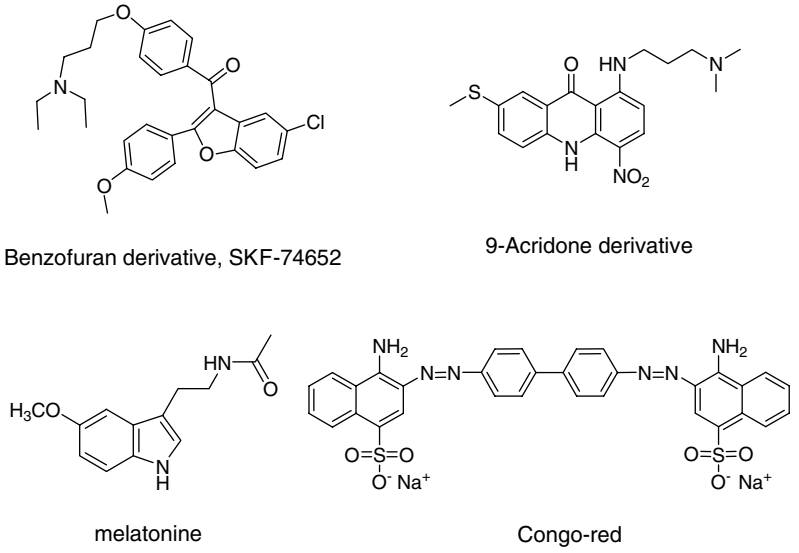

Figure 2. Structures of the effective beta-amyloid fibril aggregation inhibitors in vitro.

2. Results and discussion

2.1. Chemistry

Several possible chemical variations were considered on the basis of piperidine derivatives (Fig. 3). For binding with catalytic site of AChE, the ester with an aromatic group was designed, and for binding with peripheral site, another aromatic group was considered. As the pocket of AChE is deep, a few carbon chains as a linker were needed at the middle site between the gorge and the entrance of AChE. Several groups studied the peptidic Aβ inhibitors by modifying core regions of Aβ residue, and the numerous anti-amyloidogenic compounds have been developed.[13] Unfortunately, these peptidic amyloid aggregation inhibitors were not stable at oral administration in vivo. However, they have a hydrophobic group in common for binding with the core regions of Aβ residue.[12,13] Therefore, we considered long and linear conformation with some lipophilic groups for intercalating against Aβ peptide oligomerization. The synthetic methods for the dual action depended on the alcohols with an aromatic ring and the substituted benzoic acids, which are esterificated in the last step of the synthetic pathway.[21] Preparation of the alcohols, the key intermediate compounds **9**, **10** containing a piperidine and aromatic group, was carried out by hydride reduction using $LiAlH_4$ of the esters **7**, **8**. The esters **7**, **8** were obtained by substitution reaction of the ether containing piperidine and aromatic ring **5**, **6**. Deprotection of the *tert*-butyl carbonate group in piperidine compounds **3**, **4** gave the compounds **5**, **6**. The ethers **3**, **4** were obtained by substitution reaction of benzylbromide or benzhydrylbromide with N-protected 4-hydroxypiperidine **2**. The key intermediate compounds **9** and **10** were prepared in five steps as described in Scheme 1. All the piperidine ester derivatives **11**–**18** and **21**–**28** were synthesized with intermediate compounds **9**, **10** and the substituted benzoic acids that are commercially available. Because the reaction condition is mild and simple, there may be no problem in large scale syntheses (Scheme 2). The mixture of the corresponding substituted benzoic acid (4-chlorobenzoic acid, 4-nitrobenzoic acid, 3-fluorobenzoic acid, etc.) and compound **9** or **10** with 4-*N*,*N*-dimethylaminopyridine and *N*-[3-(dimethylamino)propyl]-*N*′-ethylcarbodiimide hydrochloride was allowed to react at room temperature. The resulting products **11**–**18** and **21**–**28** were obtained. Separately, compounds **9** or **10** were reacted with halide substituted phenyl isocyanate at *para* position in acetonitrile as solvent and then the resulting products were obtained as compounds **19**–**20** and **29**–**30** (Scheme 3). The chemical structures of all new compounds synthesized herein were fully characterized by mass analysis and proton, carbon

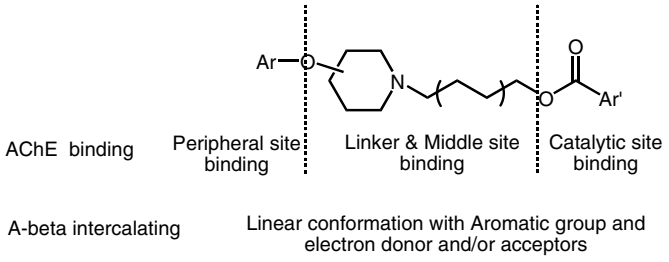

Figure 3. Design of the molecules with dual inhibitory action for AChE and amyloid-beta aggregation.

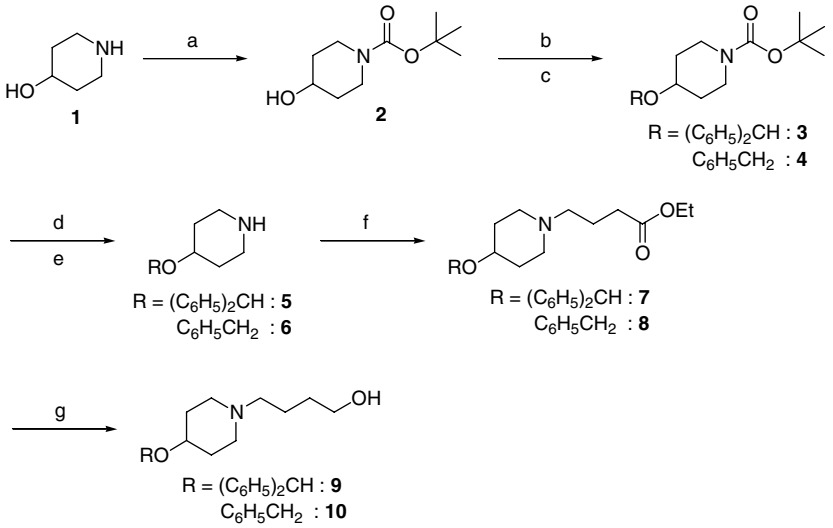

Scheme 1. Reagents and conditions: (a) Et_3N, DIBOC, $CHCl_3$, 1 h; (b) $(C_6H_5)_2CHBr$, KI (cat), Na_2CO_3 1,4-dioxane, reflux, 10 h; (c) $C_6H_5CH_2Br$, Na_2CO_3, THF, 4 h; (d) KOH, IPA, reflux, 14 h; (e) NaOH, EtOH, reflux, 6 h; (f) $NaHCO_3$, KI (cat), $Cl(CH_2)_3CO_2C_2H_5$, DMF, reflux, 4 h; (g) LAH, ether, 2 h.

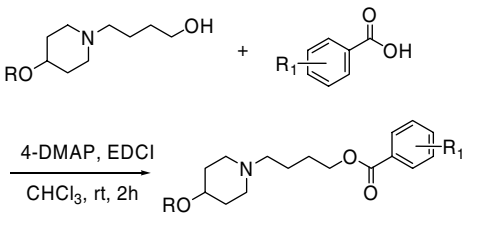

R = $(C_6H_5)_2CH$ R = $C_6H_5CH_2$
11 R_1 = H **21** R_1 = H
12 R_1 = 4-Cl **22** R_1 = 4-Cl
13 R_1 = 4-F **23** R_1 = 4-F
14 R_1 = 4-NO_2 **24** R_1 = 4-NO_2
15 R_1 = 4-*tert*-butyl **25** R_1 = 4-*tert*-butyl
16 R_1 = 4-isopropyl **26** R_1 = 4-isopropyl
17 R_1 = 3-Cl **27** R_1 = 3-Cl
18 R_1 = 3-F **28** R_1 = 3-F

Scheme 2.

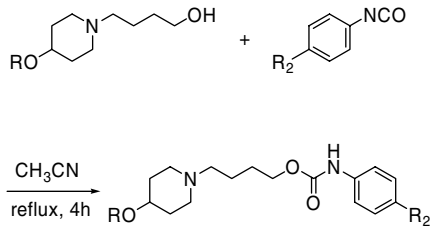

R = $(C_6H_5)_2CH_2$ R = $C_6H_5CH_2$
19 R_2 = 4-Cl **29** R_2 = 4-Cl
20 R_2 = 4-F **30** R_2 = 4-F

Scheme 3.

NMR spectroscopic data reported in the experimental section.

2.2. AChE, BChE inhibition and selectivity for AChE or BChE

To determine the therapeutic potency of the new piperidine derivatives (compounds **11**–**30**) for the AD therapeutics, their anticholinesterase activities were assayed according to Ellmann's method[22] against freshly prepared AChE from *Electrophorus electricus* and human BChE from plasma using tacrine and donepezil as reference compounds. Table 1 summarizes the data comparing AChE and BChE inhibition as well as the selectivity for AChE or BChE inhibitory activities from IC_{50} values for the new piperidine derivatives. From the IC_{50} values of compounds **11**–**30**, it appears that variations of aromatic phenyl group influenced AChE or BChE activities. In particular, compounds **11**–**20** with benzhydryl group (R) have shown AChE inhibitory activities, while compounds **21**–**30** with benzyl group showed BChE inhibitory activities. Compounds **12** and **13** possessing halogen group (R_1 = 4-Cl, 4-F) at *para* position showed best activities against AChE inhibition assay and their IC_{50} values are 0.32 and 0.84 μM, respectively. The *meta* substituted compounds **17** and **18** (R1 = 3-Cl, 3-F) showed less activity of about 1/10-fold than *para* substituted compounds. Insertion of a chlorine atom at *para* position seems to enhance binding affinity with AChE. The role of a chlorine atom at *para* position may be an anchor in the hydrophobic pocket of AChE.[23] The hydrophobic interaction between Trp279 and phenyl ring of rigid benzhydryl is more stable than flexible benzoate phenyl ring. Compound **12** could locate upside-down to the showed binding mode. We performed energy minimizing (no data), however, the result was more in preference of the suggested modeling (Figs. 4 and 5). When the compound **12** is docked with enzyme, the benzoate group could enter easier than the bulky benzhydryl group. Current studies reported that AChE is greatly reduced in specific brain regions, while BChE increases in AD patients with severe pathology. Recent evidence suggests that both AChE and BChE may have roles in the etiology and progression of AD beyond the regulation of synaptic acetylcholine levels.[24] Therefore, the synthesized compounds were screened against BChE. Compound **29** having carbamate group (X = NH) presented the best BChE inhibitory potency (IC_{50} 0.11 μM). To further characterize the pharmacological profile of the synthesized compounds, their selectivity to inhibit AChE versus BChE was determined. The selectivity for AChE of compound **12** is similar to donepezil and showed the best AChE inhibition and selectivity. Considering the selectivity for BChE, compound **29** showed the best BChE inhibition and is above 39-fold more potent than tacrine. The structural differences between compounds **12**and **19** are that R is benzhydryl or benzyl and other functional group is ester or carbamate. The peripheral anionic site (PAS) of AChE, the subsite outside of the active site gorge, mediates substrate inhibition of AChE.[25] Three aromatic amino acids located at the entrance to the active site gorge are the key residues of this subsite. The PAS of BChE, which is different from that of AChE, has weaker affinity than AChE for the typical PAS ligands and mediates substrate activation. The three aromatic residues of the AChE PAS are missing in the PAS of BChE, which is formed by two amino acid residues (Asp70 and Tyr332) in the human enzyme.[26] Recent evidence suggested that rivastigmine with carbamate group has a high BChE preference (selectivity 122 BChE, ref 26). Except some compounds, many carbamates of benzofurane, benzodioxepine, and physostigmine showed BChE preference.[27] Because compounds **12**–**20** have one more aromatic moiety than compounds **21**–**30**, their benzene rings seem to play a key role of interaction with the three aromatic residues of the AChE peripheral site and have an AChE preference. Compounds **19**, **20**, and **29**, **30** having carbamate group showed BChE inhibitory activity. Among them, compounds **29** and **30** showed high BChE preference (selectivity >400 BChE).

2.3. Molecular modeling of AChE and compound 12 with donepezil

In order to gain further insight into the mechanism of inhibition, we performed the docking study to generate the binding model for compound **12** on the basis of the existing X-ray crystal structure of AChE (PDB code: 1EVE).[28] The proposed binding model of **12** with the key residues in the gorge site is shown in Figure 4. The binding model suggests the 4-chlorobenzene of **12**

Table 1. Inhibition of AChE and BChE activities and Selectivity Ratios of the synthesized compounds

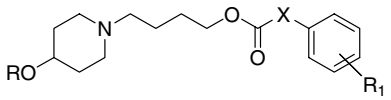

Compound	R	R_1	X	AChE inhibition[a] (μM, IC_{50})	BChE inhibition[a] (μM, IC_{50})	Selectivity[b]
11	Benzhydryl	H		1.31 ± 0.21	31.55 ± 3.53	24 AChE
12	Benzhydryl	4-Cl		0.32 ± 0.12	38.4 ± 3.72	120 AChE
13	Benzhydryl	4-F		0.84 ± 0.22	22.19 ± 1.85	26 AChE
14	Benzhydryl	4-NO_2		7.25 ± 1.31	26.83 ± 1.92	5 AChE
15	Benzhydryl	4-*tert*-Butyl		2.41 ± 0.2	78.92 ± 5.44	33 AChE
16	Benzhydryl	4-Isopropyl		3.89 ± 0.31	23.21 ± 2.73	6 AChE
17	Benzhydryl	3-Cl		3.39 ± 0.39	57.87 ± 6.23	17 AChE
18	Benzhydryl	3-F		7.72 ± 2.12	35.88 ± 3.1	5 AChE
19	Benzhydryl	4-Cl	NH	2.45 ± 0.32	13.65 ± 1.2	6 AChE
20	Benzhydryl	4-F	NH	2.45 ± 0.46	15.67 ± 1.21	6 AChE
21	Benzyl	H		>100	1.89 ± 0.56	>53 BChE
22	Benzyl	4-Cl		>100	3.52 ± 0.89	>28 BChE
23	Benzyl	4-F		>100	0.56 ± 0.21	>179 BChE
24	Benzyl	4-NO_2		>100	5.23 ± 0.78	>19 BChE
25	Benzyl	4-*tert*-Butyl		12.22 ± 1.55	15.23 ± 2.01	1.2 AChE
26	Benzyl	4-Isopropyl		14.78 ± 1.62	10.79 ± 1.86	1.4 BChE
27	Benzyl	3-Cl		>100	1.35 ± 0.35	>74 BChE
28	Benzyl	3-F		>100	1.58 ± 0.54	>63 BChE
29	Benzyl	4-Cl	NH	>100	0.25 ± 0.05	>400 BChE
30	Benzyl	4-F	NH	>100	0.78 ± 0.25	>128 BChE
Tacrine				0.15 ± 0.11	0.03 ± 0.01	5 BChE
Donepezil				0.08 ± 0.01	10.05 ± 1.72	126 AChE

The activities of AChE and BChE inhibition were screened by Ellman's method. IC_{50} is defined as the concentration of compounds that reduces by 50% of with respect to that without inhibitors. The dose–response curves have been fit by Probit analysis in StatsDirect statistical software (ver 2.5.5).

[a] Values are expressed as mean ± standard error of the mean of at least three experiments and the data showed proportional response with 95% confidence intervals.

[b] Because a smaller IC_{50} represents a higher activity, the selectivity is defined as: selectivity for AChE = IC_{50}(BChE)/IC_{50} (AChE), and selectivity for BChE = IC_{50} (AChE)/IC_{50} (BChE).

is bound to near the bottom of the gorge, and it shows parallel π–π stacking against the six-membered ring of Trp84 indole. The average distances between rings were 3.8 Å. In the middle of the gorge, the constricted region, the aliphatic alkyl chains of **12** were located as a linker and surrounded with phenyl rings of Tyr121, Phe330,

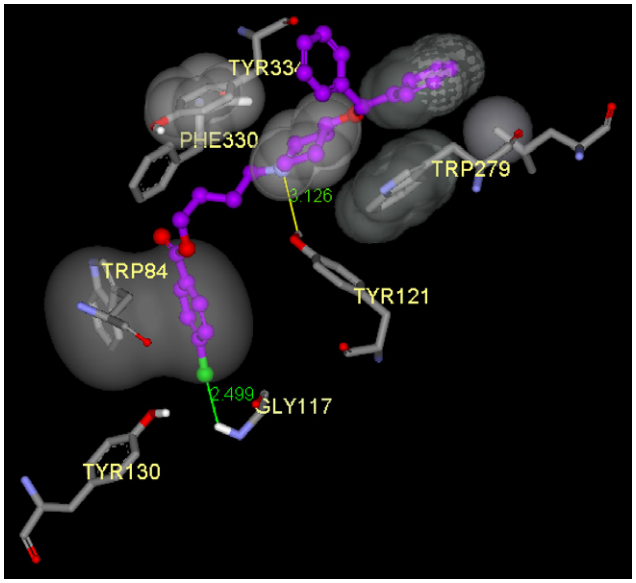

Figure 4. Proposed binding model of compound **12** with AChE. **12** is represented as a ball-and-stick model (purple) and other amino acid residues are displayed as stick model. (Color of the chloride atom is green, nitrogen is blue, hydrogen is white, and oxygen is red.)

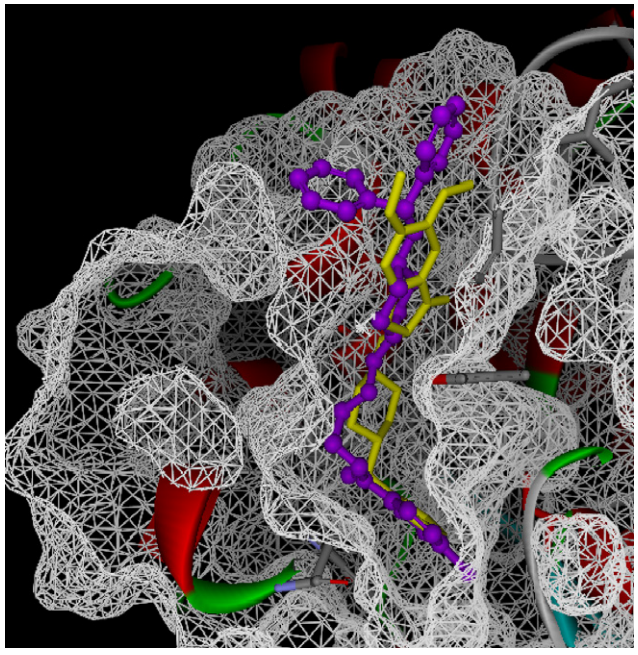

Figure 5. The superposition of compound **12** (purple) and donepezil (yellow) in the active site of AChE pocket.

and Tyr334. The nitrogen of piperidine ring could have a hydrogen bond with Tyr121 OH with the distance 3.1 Å. The piperidine ring may have van der Waals contact with Trp279 and Tyr334 (distances between the closest carbon atoms of 3.9 and 3.8 Å). At the mouth of the gorge, the benzene ring of benzhydryl group showed the hydrophobic interaction with the residues Trp279 and Leu282 (distances between the closest carbon atoms of 3.5 and 4.1 Å). In case of compound **22** possessing one benzene ring at the peripheral binding site, the hydrophobic interaction with Trp279 and Leu282 may be weak and have low potency, because of flexibility of the benzyl group. We compared donepezil (E2020) and **12** from the aspect of binding model and they were shown to be similar. Especially, the location of phenyl group to parallel π–π stacking against Trp84 was similar to **12** and donepezil. The superposition of **12** and donepezil is shown in Figure 5. In the chemical structure, both of **12** and donepezil have piperidine-nitrogen atom, but different position of piperidine-nitrogen showed the variation of potency. It seems likely that the *para*-chloro group of compound **12**plays an important role in the activity. The distance between *para*-position chlorine and hydrogen in Gly117 or hydrogen in Tyr130 is 2.5 and 3.1 Å, respectively. Therefore, the *para*-chlorine and hydrogen can take place hydrogen bonding. The evidences of halogen and hydrogen bonding were found in a lot of research results.[29] The *meta*-chloro substituent has no amino acids for hydrogen bonding nearby. Because the pocket of AChE is in the shape of a deep pitfall, **12** could locate from entrance to bottom gorge. Compound **12** was about 37-fold less potent than donepezil, because the piperidine-nitrogen of **12** (unlike donepezil which showed quaternary-π interaction with Phe330) was the about 4.6 Å distance from the piperidine-nitrogen of donepezil towards the mouth of the gorge. The backbone length of **12** is longer than donepezil. Compound **12** and donepezil have the length of 18.9 and 15.6 Å, respectively. It showed that **12** had enough length to cover the peripheral site as the active site gorge is about 20 Å deep from the mouth of gorge.[29] The benzhydryl moiety of **12** also had enough size and shape to cover the peripheral site, which was the funnel-like entrance to the gorge. The peripheral site at the mouth of the gorge has been recently postulated to regulate the Aβ assembly.[30] The result of the Aβ aggregation inhibition assay showed that **12** had good inhibitory potency. This might be due to the size differences between the benzhydryl of **12** and the dimethoxyindanone of donepezil. Thus, we suggest compound **12** could be a 'dual action' inhibitor.

2.4. Effects on the $A\beta_{1-42}$ peptide aggregation without and with AChE

To determine the amyloid-beta(1–42) aggregation inhibition of the new piperidine derivatives (compounds **11**–**30**), thioflavinT (ThT) assay was performed comparing with Congo-red, tacrine and donepezil as reference compound.[30,31] Table 2 summarizes the data for effects on the $A\beta_{1-42}$ peptide aggregation from IC_{50} values and effects on the co-aggregation of $A\beta_{1-42}$ with AChE from percent (%) inhibition at 100 and 1 μM of each compound. In the screening results of ThT assay for $A\beta_{1-42}$ aggregation inhibition, the most effective compound was **15**, followed by **12**, **18**, **13**, and **19**, and their IC_{50} values (μM) were 20.02 ± 1.84, 28.21 ± 3.12, 33.72 ± 3.23, 36.33 ± 4.1, and 37.32 ± 2.8, respectively. To further explore the dual action of these compounds, AChE-induced $A\beta_{1-42}$ aggregation inhibitory activity was examined employing the same ThT-based fluorometric assay.[30,32] In the co-aggregation study, compounds **15**and **12** were more effective than tacrine or donepezil. Considering the results, two aromatic rings, benzhydryl group of the synthesized compounds, could play a major role against $A\beta_{1-42}$ peptide aggregation inhibition. A number of inhibitors of Aβ fibril formation have been described that prevent the formation of a biologically active species of peptide. Short peptide fragments, based primarily on the central hydrophobic region of Aβ, have been proposed as being capable of preventing β-sheet formation.[33,34] SKF-74652, a representative benzofuran analogue, and 9-acridone derivatives are known as potent Aβ aggregation inhibitors (Fig. 2).[35] Because of their hydrophobic regions and

Table 2. Inhibition of $A\beta_{1-42}$ aggregation without and with AChE by the piperidine derivatives and reference compounds

Compound	$A\beta_{1-42}$ aggregation inhibition by ThT assay[a] (μM, IC_{50})	Inhibition with AChE 0.02 U[b]	
		100 μM[c] (%)	1 μM[d] (%)
11	40.33 ± 3.53	nd[e]	nd[e]
12	28.21 ± 3.12	55.5	42.4
13	36.33 ± 4.1	41.8	28.4
14	53.14 ± 5.26	nd[e]	nd[e]
15	20.02 ± 1.84	72.4	61.2
16	76.86 ± 6.4	nd[e]	nd[e]
17	91.96 ± 10.2	nd[e]	nd[e]
18	33.72 ± 3.23	52.0	41.4
19	37.32 ± 2.8	34.6	15.5
20	113.64 ± 8.9	nd[e]	nd[e]
21	105.32 ± 9.53	nd[e]	nd[e]
22	>150	nd[e]	nd[e]
23	>150	nd[e]	nd[e]
24	>150	nd[e]	nd[e]
25	78.5 ± 5.7	nd[e]	nd[e]
26	85.92 ± 6.9	nd[e]	nd[e]
27	69.4 ± 6.75	nd[e]	nd[e]
28	74.94 ± 7.4	nd[e]	nd[e]
29	>150	nd[e]	nd[e]
30	>150	nd[e]	nd[e]
Congo-red	1.65 ± 0.2	99.9	99.5
Tacrine	>150	0	0
Donepezil	86.5 ± 7.87	0	0

[a] Each value of $A\beta_{1-42}$ aggregation inhibition was from Thioflavin T (ThT) assay using fluorospectrometer. The dose–response curves have been fit by Probit analysis in StatsDirect statistical software (ver 2.5.5). The values are expressed as means ± standard error of the mean at least three experiments and the data showed proportional response with 95% confidence intervals.

[b] Co-aggregation inhibition of $A\beta_{1-42}$ and AChE 0.02 U was detected by ThT assay.

[c] The data (%) showed that the test compounds inhibited the co-aggregation at 100 μM.

[d] The data (%) showed that the test compounds inhibited the co-aggregation at 1 μM.

[e] nd, not determined.

hydrogen bond acceptors, they are capable of multiple binding for inhibition on the Aβ peptide. Other studies suggested the role of AChE not only in the hydrolysis of neurotransmitter ACh, but also in accelerating the aggregation of Aβ into amyloid fibrils (AChE-induced Aβ-fibrillogenesis).[32,36] In the recent study, the benzylethers of pyridinium-type compounds showed high activity against AChE and Aβ aggregation dual inhibition.[37] Although the benzofuran, the benzylether and the piperidine derivatives are not of the same structure, they have common hydrophobic regions, hydrogen bond acceptors, and the proper molecular length. These structural characters could give effect for multiple binding on the Aβ peptide and a further study using pharmacophore mapping and virtual screening is needed.

2.5. Neuroprotective effects on the IMR-32 cell line

The cytotoxic effect of the new piperidine derivatives was screened in human neuroblastoma cell line, IMR-32.[32,38] Table 3 represents cell viability (%) by treatment of the synthesized compounds comparing with control cells. Control cells were treated with $A\beta_{1-42}$ peptide only. When the viability of control cells became about 50% compared with standard cells (untreated peptide or inhibitors), the viability of compound treated cells was determined by MTT assay. The most neuroprotective compound was **12**, followed by **15**, donepezil, and **11**. For tacrine and **13**, cytotoxicity was found at 0.1 μmol/mL against IMR-32 cells. It is well known that tacrine has hepatotoxicity and cytotoxicity against hepatocellular carcinoma, HepG2, however, donepezil has lesser toxicity in vivo and in vitro.[39,40] In this study, tacrine has little neuroprotective effect (42.0%) against $A\beta_{1-42}$ peptide treated human neuroblastoma cells at similar level with control cells (49.1%) in vitro. On the other hand, compounds **12** (90.5%), **15** (85.2%), and donepezil (82.6%) showed good neuroprotective effect. The cytotoxic mechanism of tacrine is not clear, but it is reported that tacrine and some polycyclic aromatic compounds may be inactivating CYP1A enzymes and inhibiting drug metabolism pathway and the increased toxicity is NADPH dependent.[41] The piperidine derivatives aren't seem to be related with CYP1A enzymes by the reason that the compounds are not polycyclic compounds. Their hydrophobic aromatic group and hydrogen bond acceptor may be having neuroprotective effect. Because compound **13** has a strong electron-withdrawing fluoro group, it is likely to act as a cytotoxic factor. The exact reason for the neuroprotective effect is unknown; therefore its mechanism needs further study.

Table 3. Neuroprotective effects on the neuron cell line, IMR-32 in vitro

Compound	Cell viability (0.1 μmol/ml) (%)
Control	49.1[a]
11	80.5[b]
12	90.5
13	36.3
15	85.2
19	56.5
Tacrine	42.0
Donepezil	82.6

[a] Control group was treated with $A\beta_{1-42}$ peptide only.

[b] Test group was treated with $A\beta_{1-42}$ plus the synthesized compound or reference drugs on 0.1 μmol/mL concentration. The neuroprotective effect against neuron cells was determined by MTT assay.

3. Conclusion

We have synthesized new piperidine derivatives having dual inhibitory potency of AChE and $A\beta_{1-42}$ peptide aggregation. Compound **12** displayed the most inhibitory potency against AChE (IC_{50} = 0.32 μM) and selectivity (AChE relative to BChE) of 120 times. This contains a benzhydryl group as a peripheral site interaction unit and a phenyl ring as a catalytic site binding unit, and the two units are connected with a piperidine and alkyl chains as a linker. In the docking model, 4-chlorobenzene of **12** showed parallel π–π stacking against the indole ring of Trp84 in the bottom gorge of AChE. **29** and **30** showed high selectivity for BChE and had structure of carbamate with benzylpiperidinyl ether. Unlike AChE, the physiological function of BChE is still unclear. Therefore, the selective BChE inhibitor may be an interesting compound for the new AD therapeutic area. Compounds **12** and **15** showed good inhibition effects on $A\beta_{1-42}$ peptide oligomerization and the AChE-induced aggregation. In the molecular modeling, compound **12** had enough length to cover the mouth gorge of AChE and the benzyhydryl moiety of **12** covered the entrance to the gorge of the peripheral site in a funnel-like shape. Therefore, **12** and **15** could inhibit the AChE-induced $A\beta_{1-42}$ peptide aggregation. The obtained results are valuable for further study focusing on investigating the dual inhibitor for Alzheimer's disease therapeutics.

4. Experimental

4.1. Chemistry

Reaction progress was monitored using analytical thin-layer chromatography (TLC) on precoated Merck silica gel Kiesegel 60 F_{254} plates and the spots were detected under UV light (254 nm). The flash chromatography was conducted using silica gel 230–400 mesh. IR spectra were measured on a Jasco FT/IR-430 spectrophotometer. ^{1}H and ^{13}C NMR spectra were recorded at 300 MHz on a Bruker ARX 300 spectrometer. The chemical shifts are reported downfield in ppm (δ) relative to internal TMS, and coupling constants are reported in Hertz (Hz). Mass spectra analysis was performed on a Quattro micro MS Micromass UK mass spectrometer and recorded on an electrospray ionization mass spectrometer as the value m/z. All chemicals and solvents were purchased from Sigma–Aldrich.

4.2. *tert*-Butyl 4-hydroxypiperidine-1-carboxylate (2)

4-Hydroxypiperidine **1** (10.0 g, 98.86 mmol) was dissolved in chloroform (150 mL) and cooled at 0 °C. Triethylamine (16.5 mL, 118.63 mmol) was added above

the solution slowly and stirred for 1 h at room temperature with di-*tert*-butyl dicarbonate (DIBOC, 25.8 g, 118.63 mmol). The reaction was completed with water and the resultant solution was acidified by concentrated HCl in ice bath and extracted with chloroform. The chloroform layer was dried with anhydrous Na_2SO_4 and evaporated under reduced pressure. The flash chromatography was performed and obtained brown-yellowish solid product **2** (yield 83%). Mp: 56–59 °C. IR (KBr): 3485, 2934, 1671, 1434, 1170 cm^{-1}. ^1H NMR ($CDCl_3$): δ 1.52 (s, 9H), 1.81–1.91 (m, 4H), 2.95–3.08 (m, 2H), 3.83–3.89 (m, 3H). ^{13}C NMR ($CDCl_3$): δ 28.3, 34.1, 41.2, 67.6, 79.5, 154.7.

4.3. General procedure for the preparation of derivatives 3 and 4

To 90 mL of 1,4-dioxane were added compound **2** (9.7 g, 26.4 mmol), Na_2CO_3 (3.6 g, 34.38 mmol), KI (catalyst) and diphenylbromomethane (8.5 g, 34.28 mmol), or benzylbromide (1.3 equiv, 34.28 mmol). The mixture was refluxed for 10 h and then the resultant was evaporated. The concentrated solution was poured into water and extracted with methylene chloride. The methylene chloride layer was dried with anhydrous Na_2SO_4 and evaporated under reduced pressure. The flash chromatography was performed and obtained liquid products.

4.3.1. *tert*-Butyl 4-(benzhydryloxy)piperidine-1-carboxylate (3). Yield 72%, brownish liquid, IR (NaCl): 2941, 1732, 1492, 1452, 1180, 1071 cm^{-1}. ^1H NMR ($CDCl_3$): δ 1.53 (s, 9H), 1.57–1.86 (m, 2H), 3.04–3.17 (m, 2H), 3.53–3.61 (m, 1H), 3.67–3.79 (m, 2H), 5.51 (s, 1H), 7.18–7.36 (m, 10H). ^{13}C NMR ($CDCl_3$): δ 28.3, 31.0, 71.8, 80.1, 126.8, 126.9, 127.2, 128.2, 142.5, 184.0.

4.3.2. *tert*-Butyl 4-(benzyloxy)piperidine-1-carboxylate (4). Yield 82%, yellowish liquid, IR (NaCl): 3125, 1750, 1510, 1180, 1060 cm^{-1}. ^1H NMR ($CDCl_3$): δ 1.53 (s, 9H), 1.61–1.82 (m, 2H), 3.04–3.17 (m, 2H), 3.58 (m, 1H), 3.67–3.79 (m, 2H), 5.51 (s, 1H), 7.21–7.38 (m, 5H).

4.4. General procedure for the preparation of derivatives 5 and 6

To the dried isopropyl alcohol was added compound **3** or **4** (1 equiv) and KOH (10 equiv). The mixture was refluxed for 14 h, cooled down to room temperature, and distilled water was added for ending the reaction. The resultant was extracted with chloroform and evaporated under reduced pressure. The flash chromatography was performed and obtained liquid product.

4.4.1. 4-Benzhydryloxypiperidine (5). Yield 70%, yellowish liquid, ^1H NMR ($CDCl_3$): δ 1.49–1.62 (m, 2H), 1.88–1.96 (m, 2H), 2.48–2.62 (m, 2H), 3.04–3.12 (m, 2H), 3.45–3.49 (m, 2H), 5.54 (s, 1H), 7.21–7.40 (m, 10H). ^{13}C NMR ($CDCl_3$): δ 33.06, 44.3, 73.0, 79.8, 127.0, 127.2, 128.2, 142.7; ESI-MS: 268.1 (M+1).

4.4.2. 4-Benzyloxypiperidine (6). Yield 80%, yellowish liquid, ^1H NMR ($CDCl_3$): δ 1.65–2.05 (m, 4H), 3.04–3.12 (m, 2H), 3.31–3.42 (m, 2H), 3.45 (m, 1H), 5.24 (s, 1H), 7.28–7.36 (m, 5H).

4.5. General procedure for the preparation of derivatives 7 and 8

To 12–28 mL of *N*,*N*-dimethylformamide (DMF) were added compound **5** or **6** (1.0 g, 3.74 mmol), $NaHCO_3$ (1.42 g), potassium iodide (catalyst), and ethyl-4-chlorobutyrate (5.61 or 7.84 mmol). The mixture was refluxed for 4 h and cooled down to room temperature. The resulting solution was extracted with chloroform and washed with water. The organic layer was dried over anhydrous Na_2SO_4 and evaporated under reduced pressure. The flash chromatography was performed and obtained liquid product.

4.5.1. Ethyl-4-[4-(benzhydryloxy)piperidino]butanoate (7). Yield 66%, yellowish liquid, ^1H NMR ($CDCl_3$): δ 1.26 (t, J = 7.2 Hz, 3H), 1.77–1.93 (m, 6H), 2.05–2.12 (m, 2H), 2.28–2.33 (m, 4H), 2.69–2.77 (m, 2H), 3.38–3.46 (m, 1H), 4.14 (q, J = 7.2 Hz, 2H), 5.53 (s, 1H), 7.23–7.37 (m, 10H). ^{13}C NMR ($CDCl_3$): δ 14.2, 22.1, 22.4, 27.6, 27.7, 31.0, 31.3, 32.3, 51.0, 57.6, 60.2, 60.4, 62.0, 72.5, 68.4, 79.9, 127.0, 127.2, 128.2, 142.8, 173.5, 177.6; ESI-MS: 382.2 (M+1).

4.5.2. Ethyl 4-[4-(benzyloxy)piperidino]butanoate (8). Yield 82%, yellowish liquid, ^1H NMR ($CDCl_3$): δ 1.22 (t, J = 7.2 Hz, 3H), 1.67–1.91 (m, 6H), 2.09–2.19 (m, 2H), 2.27–2.36 (m, 4H), 2.72–2.78 (m, 2H), 3.38–3.42 (m, 1H), 4.10 (q, J = 7.2 Hz, 2H), 4.51 (s, 2H), 7.23–7.34 (m, 5H). ^{13}C NMR ($CDCl_3$): δ 14.1, 22.4, 31.2, 32.3, 51.1, 57.5, 60.1, 69.5, 127.3, 128.2, 138.9, 173.5; ESI-MS: 306.2 (M+1).

4.6. General procedure for the preparation of derivatives 9 and 10

The compound **7** or **8** (1.0 g, 2.62 or 3.27 mmol) was dissolved in 10 mL of ether and cooled in an ice bath. $LiAlH_4$ (0.2 or 0.25 g, 5.24 or 6.54 mmol) was added to the solution slowly. The mixture was stirred at room temperature for 2 h and added water to end the reaction. The resulting solution was then extracted with ether and washed with water. The organic layer was dried over magnesium sulfate and evaporated under reduced pressure. The flash chromatography was performed and obtained liquid product.

4.6.1. 4-[4-(Benzhydryloxy)piperidino]-1-butanol (9). Yield 43%, yellowish liquid, ^1H NMR ($CDCl_3$): δ 1.68–1.77 (m, 4H), 1.78–1.94 (m, 4H), 2.27–2.38 (m, 4H), 2.76–2.79 (m, 2H), 3.45–3.58 (m, 3H), 5.51 (s, 1H), 7.23–7.36 (m, 10H). ^{13}C NMR ($CDCl_3$): δ 25.7, 30.5, 32.6, 58.4, 62.6, 80.1, 127.0, 127.2, 128.2, 142.7; ESI-MS: 340.2 (M+1).

4.6.2. 4-[4-(Benzyloxy)piperidino]-1-butanol (10). Yield 83%, yellowish liquid, ^1H NMR ($CDCl_3$): δ 1.62–1.76 (m, 6H), 1.84–1.91 (m, 2H), 2.21–2.31 (m, 4H), 2.70–2.76 (m, 2H), 3.42–3.56 (m, 3H), 4.48 (s, 2H), 7.19–7.30 (m, 5H). ^{13}C NMR ($CDCl_3$): δ 25.8, 30.4, 32.7,

50.4, 50.5, 58.4, 62.6, 69.9, 127.3, 128.3, 138.8; ESI-MS: 266.1 (M+1).

4.7. General procedure for the preparation of derivatives 11–18 and 21–28

To 15 mL of chloroform was added compound **9** or **10** (0.619 or 1.135 mmol), each of benzoic acid derivatives (1.5 equiv), 4-dimethylaminopyridine (3 equiv), and 1-[3-(dimethylamino)propyl]-3-ethylcarboimide hydrochloric acid (1.1 equiv). The mixture was allowed to react at room temperature for 2 h and added water to end the reaction. The resulting solution was acidified with 1 N HCl and extracted using chloroform. An organic layer was washed with 1 N NaOH, dried over magnesium sulfate, and evaporated under reduced pressure. The flash chromatography was performed and obtained each product.

4.7.1. 4-[4-(Benzhydryloxy)piperidino]butyl benzoate (11). Yield 63%, yellowish liquid, ^{1}H NMR ($CDCl_3$): δ 1.67–1.91 (m, 8H), 2.12–2.20 (m, 2H), 2.40 (t, J = 7.4 Hz, 2H), 2.77–2.80 (m, 2H), 3.44–3.50 (m, 1H), 4.35 (t, J = 6.4 Hz, 2H), 5.54 (s, 1H), 7.25–7.37 (m, 10H), 7.42–7.47 (m, 2H), 7.54–7.57 (m, 1H), 8.05 (d, J = 7.2 Hz, 2H). ^{13}C NMR ($CDCl_3$): δ 23.7, 26.8, 31.2, 51.0, 58.1, 64.8, 79.9, 127.0, 127.2, 128.2, 129.5, 130.3, 132.8, 142.7; ESI-MS: 444.2 (M+1).

4.7.2. 4-[4-(Benzhydryloxy)piperidino]butyl-4-chlorobenzoate (12). Yield 71%, yellowish liquid, ^{1}H NMR ($CDCl_3$): δ 1.62–1.90 (m, 8H), 2.14–2.22 (m, 2H), 2.39 (t, J = 7.4 Hz, 2H), 2.74 (m, 2H), 3.45–3.51 (m, 1H), 4.3 (t, J = 6.3 Hz, 2H), 5.53 (s, 1H), 7.27–7.37 (m, 10H), 7.41 (d, J = 8.5 Hz, 2H), 7.97 (d, J = 8.5 Hz, 2H). ^{13}C NMR ($CDCl_3$): δ 23.7, 26.7, 31.3, 51.1, 58.1, 65.1, 80.0, 127.2, 127.6, 128.2, 128.6, 128.8, 130.9, 139.2, 142.8, 165.7; ESI-MS: 478.2 (M+1).

4.7.3. 4-[4-(Benzhydryloxy)piperidino]butyl 4-fluorobenzoate (13). Yield 74%, yellowish liquid, ^{1}H NMR ($CDCl_3$): δ 1.61–1.89 (m, 8H), 2.11–2.14 (m, 2H), 2.34 (t, J = 7.4 Hz, 2H), 2.69–2.77 (m, 2H), 3.38–3.45 (m, 1H), 4.29 (t, J = 6.4 Hz, 2H), 5.50 (s, 1H), 7.07 (dd, J = 8.9, 8.3 Hz, 2H), 7.21–7.39 (m, 10H), 8.02 (dd, J = 8.9, 5.5 Hz, 2H). ^{13}C NMR ($CDCl_3$): δ 23.7, 26.7, 31.3, 51.1, 58.0, 64.9, 79.9, 115.2, 115.5, 126.5, 127.0, 127.2, 128.2, 131.9, 132.0, 142.8, 163.9, 165.5; 167.2; ESI-MS: 462.2 (M+1).

4.7.4. 4-[4-(Benzhydryloxy)piperidino]butyl-4-nitrobenzoate (14). Yield 76%, yellowish liquid, ^{1}H NMR ($CDCl_3$): δ 1.65–1.89 (m, 8H), 2.06–2.16 (m, 2H), 2.39 (t, J = 7.4 Hz, 2H), 2.74–2.77 (m, 2H), 3.45–3.48 (m, 1H), 4.40 (t, J = 6.4 Hz, 2H), 5.53 (s, 1H), 7.23–7.37 (m, 12H), 8.21 (d, J = 8.8 Hz, 2H), 8.29 (d, J = 8.7 Hz, 2H). ^{13}C NMR ($CDCl_3$): δ 23.6, 26.6, 31.2, 51.0, 57.9, 65.7, 72.3, 80.0, 126.5, 122.7, 123.4, 126.7, 127.0, 127.2, 127.8, 128.2, 128.5, 129.9, 130.6, 135.7, 142.7, 150.4, 164.6; ESI-MS: 489.2 (M+1).

4.7.5. 4-[4-(Benzhydryloxy)piperidino]butyl-4-(*tert*-butyl)benzoate (15). Yield 96%, yellowish liquid, ^{1}H NMR ($CDCl_3$): δ 1.41 (s, 9H), 1.72–1.86 (m, 8H), 2.05–2.15 (m, 2H), 2.34 (t, J = 7.4 Hz, 2H), 2.71–2.77 (m, 2H), 3.39–3.47 (m, 1H), 4.3 (t, J = 6.4 Hz, 2H), 5.51 (s, 1H), 7.21–7.37 (m, 10H), 7.42 (d, J = 8.3 Hz, 2H), 7.96 (d, J = 8.3 Hz, 2H). ^{13}C NMR ($CDCl_3$): δ 23.7, 26.8, 31.0, 31.3, 35.0, 51.1, 58.1, 64.6, 79.9, 125.2, 127.0, 127.2, 127.6, 128.2, 129.3, 142.8, 165.7; ESI-MS: 500.3 (M+1).

4.7.6. 4-[4-(Benzhydryloxy)piperidino]butyl 4-isopropylbenzoate (16). Yield 66%, yellowish liquid, ^{1}H NMR ($CDCl_3$): δ 1.24 (d, J = 7.2 Hz, 6H), 1.58–1.86 (m, 8H), 2.04–2.18 (m, 2H), 2.34 (t, J = 7.6 Hz, 2H), 2.72–2.78 (m, 2H), 2.90–2.97 (m, 1H), 3.46–3.40 (m, 1H), 4.28 (t, J = 6.4 Hz, 2H), 5.50 (s, 1H), 7.19–7.38 (m, 12H), 7.93 (d, J = 8.4 Hz, 2H). ^{13}C NMR ($CDCl_3$): δ 23.6, 23.7, 26.7, 31.3, 34.1, 40.8, 51.0, 58.0, 64.5, 72.4, 89.9, 126.3, 126.9, 127.1, 127.9, 128.1, 129.5, 142.7, 154.1, 166.5; ESI-MS: 486.2 (M+1).

4.7.7. 4-[4-(Benzhydryloxy)piperidino]butyl 3-chlorobenzoate (17). Yield 33%, yellowish liquid, ^{1}H NMR ($CDCl_3$): δ 1.57–1.92 (m, 8H), 2.10–2.18 (m, 2H), 2.34 (t, J = 7.4 Hz, 2H), 2.73–2.79 (m, 2H), 3.41–3.48 (m, 1H), 4.31 (t, J = 6.4 Hz, 2H), 5.50 (s, 1H), 7.20–7.39 (m, 11H), 7.50 (d, J = 8.0 Hz, 1H), 7.89 (d, J = 7.6 Hz, 1H), 7.98 (s, 1H). ^{13}C NMR ($CDCl_3$): δ 23.7, 26.7, 31.3, 51.1, 58.0, 65.2, 72.3, 79.9, 116.2, 116.5, 119.7, 119.9, 125.2, 127.0, 127.2, 127.6, 128.2, 129.5, 129.6, 132.1, 132.8, 134.4, 142.8, 165.3; ESI-MS: 478.2 (M+1).

4.7.8. 4-[4-(Benzhydryloxy)piperidino]butyl 3-fluorobenzoate (18). Yield 14%, yellowish liquid, ^{1}H NMR ($CDCl_3$): δ 1.66–1.92 (m, 8H), 2.17–2.24 (m, 2H), 2.40 (t, J = 7.2 Hz, 2H), 2.76–2.82 (m, 2H), 3.44–3.49 (m, 1H), 4.35 (t, J = 6.4 Hz, 2H), 5.53 (s, 1H), 7.23–7.43 (m, 12H), 7.72(d, J = 7.7 Hz, 1H), 7.84 (d, J = 7.7 Hz, 1H).^{13}C NMR ($CDCl_3$): δ 23.7, 26.7, 31.3, 51.1, 58.0, 65.2, 80.0, 116.2, 116.5, 119.7, 120.0, 125.2, 127.0, 127.2, 128.2, 129.8, 129.9, 132.5, 132.6, 142.8, 160.8, 165.4; ESI-MS: 462.2 (M+1).

4.7.9. 4-[4-(Benzyloxy)piperidino]butyl benzoate (21). Yield 69%, yellowish liquid, ^{1}H NMR ($CDCl_3$): δ 1.58–1.79 (m, 6H), 1.88–1.96 (m, 2H), 2.08–2.16 (m, 2H), 2.35 (t, J = 7.4 Hz, 2H), 2.74–2.78 (m, 2H), 3.36–3.44 (m, 1H), 4.30 (t, J = 6.4 Hz, 2H), 4.51 (s, 2H), 7.21–7.33 (m, 5H), 7.38–7.45 (m, 2H), 7.50–7.54 (m, 1H), 8.01 (d, J = 9.6 Hz, 2H).^{13}C NMR ($CDCl_3$): δ 23.8, 26.8, 31.2, 51.1, 58.1, 64.8, 69.6, 127.4, 128.3, 129.5, 130.3, 132.8, 138.9, 166.6; ESI-MS: 368.2 (M+1).

4.7.10. 4-[4-(Benzyloxy)piperidino]butyl-4-chlorobenzoate (22). Yield 61%, yellowish liquid, ^{1}H NMR ($CDCl_3$): δ 1.68–1.94 (m, 8H), 2.15–2.22 (m, 2H), 2.40 (t, J = 7.4 Hz, 2H), 2.78–2.84 (m, 2H), 3.42–3.46 (m, 1H), 4.34 (t, J = 6.4 Hz, 2H), 4.56 (s, 2H), 7.28–7.37 (m, 5H), 7.42 (d, J = 8.4 Hz, 2H), 7.98 (d, J = 8.4 Hz, 2H). ^{13}C NMR ($CDCl_3$): δ 22.2, 23.7, 25.6, 26.8, 31.2, 51.1, 58.1, 65.1, 69.6, 127.3, 127.4, 128.3, 128.6, 128.8, 130.9, 133.6, 138.9, 139.2; ESI-MS: 402.1 (M+1).

4.7.11. 4-[4-(Benzyloxy)piperidino]butyl-4-fluorobenzoate (23). Yield 63%, yellowish liquid, ^{1}H NMR ($CDCl_3$): δ

1.61–1.78 (m, 6H), 1.84–1.90 (m, 2H), 2.10–2.16 (m, 2H), 2.34 (t, J = 7.6 Hz, 2H), 2.71–2.78 (m, 2H), 3.38–3.44 (m, 1H), 4.29 (t, J = 6.8 Hz, 2H), 4.51 (s, 2H), 7.07 (dd, J = 8.7, 8.4 Hz, 2H), 7.21–7.34 (m, 5H), 8.02 (dd, J = 8.9, 8.7 Hz, 2H).^{13}C NMR ($CDCl_3$): δ 23.7, 26.8, 31.2, 51.1, 58.1, 65.0, 69.6, 74.3, 115.2, 115.5, 126.5, 126.6, 127.4, 128.3, 131.9, 138.9, 164.0, 165.6, 167.3, 184.9; ESI-MS: 386.2 (M+1).

4.7.12. 4-[4-(Benzyloxy)piperidino]butyl-4-nitrobenzoate (24). Yield 64%, yellowish liquid, ^{1}H NMR ($CDCl_3$): δ 1.64–1.91 (m, 8H), 2.12–2.18 (m, 2H), 2.40 (t, J = 7.4 Hz, 2H), 2.76–2.82 (m, 2H), 3.42–3.48 (m, 1H), 4.40 (t, J = 6.4 Hz, 2H), 4.55 (s, 2H), 7.27–7.36 (m, 5H), 8.21 (d, J = 8.6 Hz, 2H), 8.29 (d, J = 8.6 Hz, 2H). ^{13}C NMR ($CDCl_3$): δ 23.7, 26.7, 31.2, 51.1, 58.0, 65.8, 69.6, 123.4, 127.4, 128.3, 130.6, 135.7, 138.8, 150.4, 164.6, 184.8; ESI-MS: 413.2 (M+1).

4.7.13. 4-[4-(Benzyloxy)piperidino]butyl-4-(*tert*-butyl)-benzoate (25). Yield 76%, yellowish liquid, ^{1}H NMR ($CDCl_3$): δ 1.32 (s, 9H), 1.64–1.78 (m, 6H), 1.86–1.92 (m, 2H), 2.08–2.14 (m, 2H), 2.35 (t, J = 7.4 Hz, 2H), 2.72–2.77 (m, 2H), 3.37–3.41 (m, 1H), 4.29 (t, J = 6.4 Hz, 2H), 4.51 (s, 2H), 7.23–7.36 (m, 5H), 7.42 (d, J = 8.0 Hz, 2H), 7.94 (d, J = 8.0 Hz, 2H). ^{13}C NMR ($CDCl_3$): δ 23.7, 26.8, 31.1, 31.2, 35.0, 51.2, 57.4, 58.1, 64.6, 69.6, 125.2, 127.3, 127.4, 127.6, 128.3, 129.3, 138.9, 156.4, 166.6; ESI-MS: 424.2 (M+1).

4.7.14. 4-[4-(Benzyloxy)piperidino]butyl-4-isopropylbenzoate (26). Yield 64%, yellowish liquid, ^{1}H NMR ($CDCl_3$): δ 1.24 (d, J = 7.3 Hz, 6H), 1.63–1.77 (m, 6H), 1.80–1.94 (m, 2H), 2.10–2.14 (m, 2H), 2.39 (t, J = 7.4 Hz, 2H), 2.76–2.81 (m, 2H), 2.90–2.97 (m, 1H), 3.38–3.44 (m, 1H), 4.33 (t, J = 6.4 Hz, 2H), 4.56 (s, 2H), 7.29–7.37 (m, 7H), 7.94 (d, J = 7.9 Hz, 2H). ^{13}C NMR ($CDCl_3$): δ 23.6, 23.7, 26.8, 31.2, 34.2, 51.2, 58.1, 64.6, 69.6, 126.4, 127.3, 127.4, 128.0, 128.3, 129.6, 138.9, 154.2, 166.6; ESI-MS: 410.2 (M+1).

4.7.15. 4-[4-(Benzyloxy)piperidino]butyl-3-chlorobenzoate (27). Yield 47%, yellowish liquid, ^{1}H NMR ($CDCl_3$): δ 1.57–1.77 (m, 6H), 1.89–1.96 (m, 2H), 2.08–2.14 (m, 2H), 2.31 (t, J = 7.4 Hz, 2H), 2.71–2.78 (m, 2H), 3.36–3.42 (m, 1H), 4.30 (t, J = 6.4 Hz, 2H), 4.51 (s, 2H), 7.21–7.38 (m, 6H), 7.48 (d, J = 8.0 Hz, 1H), 7.86 (d, J = 7.6 Hz, 1H), 7.94 (s, 1H). ^{13}C NMR ($CDCl_3$): δ 23.7, 26.7, 31.2, 51.1, 58.0, 65.3, 67.3, 67.4, 69.6, 74.3, 127.3, 127.4, 127.6, 128.3, 129.6, 132.1, 132.8, 134.4, 138.9, 165.3; ESI-MS: 402.1 (M+1).

4.7.16. 4-[4-(Benzyloxy)piperidino]butyl-3-fluorobenzoate (28). Yield 48%, yellowish liquid, ^{1}H NMR ($CDCl_3$): δ 1.64–1.79 (m, 6H), 1.89–1.94 (m, 2H), 2.08–2.17 (m, 2H), 2.35 (t, J = 7.4 Hz, 2H), 2.73–2.84 (m, 2H), 3.39–3.44 (m, 1H), 4.31 (t, J = 6.4 Hz, 2H), 4.51 (s, 2H), 7.24–7.66 (m, 7H), 7.80 (ddd, J = 8.0, 2.5, 1.5 Hz, 1H), 7.79 (d, J = 8.0 Hz, 1H). ^{13}C NMR ($CDCl_3$): δ 23.7, 26.7, 31.2, 51.1, 58.0, 65.2, 69.6, 116.2, 116.5, 119.7, 120.0, 125.2, 127.3, 127.4, 128.3, 129.8, 129.9, 132.4, 132.5, 138.9, 160.8, 164.1, 165.4; ESI-MS: 386.2 (M+1).

4.8. General procedure for the preparation of derivatives 19–20 and 29–30

To 25 mL of acetonitrile was added compound **9** or **10** (1.945 or 2.658 mmol), 4-chloro- or fluoro-phenyl isocyanate (1.2 equiv). The mixture was refluxed for 4 h, cooled, and evaporated under reduced pressure. The resulting solution was then extracted by using water and chloroform. An organic layer was dried with magnesium sulfate, and evaporated under reduced pressure. The flash chromatography was performed and obtained product.

4.8.1. 4-[4-(Benzhydryloxy)piperidino]butyl-*N*-(4-chlorophenyl)carbamate (19). Yield 24%, yellowish liquid, ^{1}H NMR ($CDCl_3$): δ 1.68–1.94 (m, 6H), 2.04–2.12 (m, 2H), 2.22–2.28 (m, 2H), 2.43 (t, J = 7.2 Hz, 2H), 2.76–2.82 (m, 2H), 3.47–3.51 (m, 1H), 4.18 (t, J = 5.4 Hz, 2H), 5.52 (s, 1H), 6.85 (s, 1H), 7.24–7.43 (m, 14H). ^{13}C NMR ($CDCl_3$): δ 20.9, 26.4, 26.5, 30.6, 57.5, 57.8, 60.7, 64.0, 64.6, 80.2, 126.9, 127.0, 127.3, 128.3, 128.9, 136.6, 142.5, 142.4, 142.6, 152.0, 153.4, 171.1; ESI-MS: 493.2 (M+1).

4.8.2. 4-[4-(Benzhydryloxy)piperidino]butyl-*N*-(4-fluorophenyl)carbamate (20). Yield 24%, yellowish liquid, ^{1}H NMR ($CDCl_3$): δ 1.66–1.92 (m, 6H), 1.81–1.97 (m, 2H), 2.09–2.16 (m, 2H), 2.31 (t, J = 6.1 Hz, 2H), 2.74–2.82 (m, 2H), 3.39–3.42 (m, 1H), 4.12 (t, J = 5.6 Hz, 2H), 5.49 (s, 1H), 6.67 (s, 1H), 6.98 (t, J = 8.8 Hz, 2H), 7.14–7.25 (m, 12H). ^{13}C NMR ($CDCl_3$): δ 22.6, 26.5, 29.6, 30.2, 50.3, 57.6, 64.1, 64.5, 80.2, 115.3, 115.6, 120.2, 126.9, 127.3, 128.2, 128.3, 133.9, 138.6, 142.5, 142.6, 153.7, 171.1; ESI-MS: 477.2 (M+1).

4.8.3. 4-[4-(Benzyloxy)piperidino]butyl-*N*-(4-chlorophenyl)carbamate (29). Yield 61%, yellowish liquid, ^{1}H NMR ($CDCl_3$): δ 1.53–1.69 (m, 6H), 1.89–1.99 (m, 2H), 2.08–2.16 (m, 2H), 2.32 (t, J = 7.2 Hz, 2H), 2.68–2.74 (m, 2H), 3.38–3.43 (m, 1H), 4.14 (t, J = 6.1 Hz, 2H), 4.51 (s, 2H), 6.97 (s, 1H), 7.21–7.32 (m, 9H).^{13}C NMR ($CDCl_3$): δ 23.2, 26.8, 30.8, 50.8, 57.7, 64.9, 69.6, 73.8, 119.8, 127.4, 128.0, 128.1, 128.3, 128.9, 136.5, 138.7, 151.2, 153.4, 174.6, 184.9; ESI-MS: 417.1 (M+1).

4.8.4. 4-[4-(Benzyloxy)piperidino]butyl-*N*-(4-fluorophenyl)carbamate (30). Yield 48%, yellowish liquid, ^{1}H NMR ($CDCl_3$): δ 1.59–1.71 (m, 6H), 1.88–1.94 (m, 2H), 2.12–2.18 (m, 2H), 2.36 (t, J = 7.2 Hz, 2H), 2.78–2.88 (m, 2H), 3.42–3.48 (m, 1H), 4.18 (t, J = 6.1 Hz, 2H), 4.56 (s, 2H), 7.02 (t, J = 8.6 Hz, 2H); 7.28–7.36 (m, 8H). ^{13}C NMR ($CDCl_3$): δ 23.1, 26.8, 30.8, 50.8, 53.3, 57.7, 64.7, 69.5, 73.8, 73.9, 115.2, 115.5, 120.3, 127.3, 128.1, 133.9, 138.6, 153.8, 157.1, 160.3, 184.5; ESI-MS: 401.2 (M+1).

4.9. AChE (or BChE) inhibition assay in vitro

Inhibitory activity against AChE (or BChE) was evaluated at 37 °C by the colorimetric method reported by Ellman et al.[22] The final concentration containing test compound of the assay solution consisted of 0.1 M

sodium phosphate buffer (pH 8.0), 0.3 mM 5,5′-dithiobis-2-nitrobenzoic acid (DTNB, Ellman's reagent), 0.02 U of AChE from *Electrophorus electricus* (or 0.01 U BChE from human serum, Sigma Chemical Co.), and 0.5 mM acetylthiocholine iodide (or 0.5 mM butyrylthiocholine) as substrate of the enzymatic reaction, respectively. The assay solutions except substrate were preincubated with the enzyme for 10 min at 37 °C. After preincubation, the substrate was added. The absorbance changes at 405 nm were recorded for 5 min with a microplate reader GENios F129004 (Tecan Ltd, Austria). The AChE inhibition (or BChE inhibition, IC_{50}) was determined for each compound. Each assay was run in triplicate and each reaction was repeated at least three independent times. The dose–response curves have been fit by Probit analysis in StatsDirect statistical software (ver 2.5.5) and the data showed proportional response with 95% confidence intervals.

4.10. Molecular modeling

Molecular modeling studies were performed on Silicon Graphics Octane2 R12000 workstation by using Cerius2 (version 4.10) and InsightII (version 2000.2) which were molecular modeling software packages. To determine the binding model, we used Cerius2. On the other hand, to get an insight into the binding mode of known ligands from the X-ray crystal structures, we used InsightII and performed structure alignments for reported AChE complex structures and their PDB codes were 1EVE, 1GPK, 1GPN, 2ACE, and 1ODC. In order to obtain a binding model of compound **12** in the active site of AChE, we performed the following steps. First, the 3D structure of **12** was minimized by using CFF1.02 which was available in Cerius2, and atomic charges were assigned by CFF1.02. We generated conformationally diverse 3D structures of **12** and chose one of the structures which had a conformationally similar structure to donepezil which bound at the active site of AChE structure (1EVE). Second, the protein structure was modeled by adding hydrogen atom followed by 'the templates for protein residues' in Cerius2, and all water molecules were removed. Third, to designate an initial position of **12** in the active site, we used donepezil as a template structure from 1EVE. We manually set the initial position of 4-chlorobenzene of **12** to be overlapped with the benzyl ring of donepezil. Lastly, energy minimization was performed to obtain a binding mode of **12** to the active site in AChE. For parameters, we set 'Smart Minimizer,' as an energy minimization method which was available in Cerius2, and set the convergence criteria to 5000 cycles with RMSD 0.1 cal/mol. We also set the ligand to be flexible to move and the protein to be rigid.

4.11. Inhibition of $A\beta_{1-42}$ peptide aggregation (Thioflavin T-based fluorometric assay)

$A\beta_{1-42}$ peptide (American Peptide Company, USA) was dissolved in DMSO to obtain a 2.3 mM solution. Aliquots of $A\beta_{1-42}$ in DMSO were then incubated for 16 h at 37 °C in 0.215 M sodium phosphate buffer (pH 8.0) at a final Aβ concentration of 20 μM in the presence or absence of test inhibitors. To quantify amyloid fibril formation, thioflavin T (ThT) fluorescence method was used.[30,31] Analyses were performed with an Infinite F200 (Tecan Ltd, Austria) and fluorescence was measured at 450 nm (λ excitation, slit width 5 nm) and 490 nm (λ emission, slit width 10 nm). To determine amyloid fibril formation, after incubation, to the solution (20 μL) containing Aβ or Aβ plus inhibitors with 0.01 M sodium phosphate buffer (pH 8.0) was added 5 μM ThT 200 μL. Each assay was run in triplicate and each reaction was repeated at least three independent times. The fluorescence intensities were recorded, and the percent aggregation was calculated by the following equation: $100 - \{(IFi - IFb)/(IFo - IFb) \times 100\}$ where IFi, IFo and IFb are the fluorescence intensities obtained for $A\beta_{1-42}$ aggregation in the presence of inhibitors, in the absence of inhibitors and the blanks, respectively. The IC_{50} is defined as the concentration of compounds that reduces by 50% of with respect to that without inhibitors. The dose–response curves have been fit by Probit analysis in StatsDirect statistical software (ver 2.5.5) and the data showed proportional response with 95% confidence intervals.

4.12. Inhibition of AChE-induced $A\beta_{1-42}$ peptide aggregation assay

For co-incubation experiments,[30,32] of $A\beta_{1-42}$ peptide (American Peptide Company, USA) and AChE from *Electrophorus electricus*, the mixtures of $A\beta_{1-42}$ peptide and AChE in presence or absence of the test inhibitors were incubated for 6 h at 37 °C. The final concentrations of Aβ (dissolved in DMSO and diluted 0.215 M sodium phosphate buffer, pH 8.0) and AChE (dissolved in 0.1 M sodium phosphate buffer, pH 8.0) are 20 μM and 0.02 U, respectively. To analyze co-aggregation inhibition, the ThT fluorescence method was used[30,31] and the fluorescence was measured at 450 nm (λ excitation, slit width 5 nm) and 490 nm (λ emission, slit width 10 nm). After co-incubation, to the mixture solutions of 20 μL was added 5 μM ThT 200 μL. Each assay was run in triplicate and each reaction was repeated at least three independent times.

4.13. Cell viability

IMR-32, human neuroblastoma cells were obtained from the American Type Culture Collection (Rockville, MD). The cells were cultured in Minimum Essential Medium with Earle's salt with L-glutamine (EMEM), 10% fetal bovine serum, and 1% penicillin/streptomycin in a highly humidified atmosphere having 5% CO_2at 37 °C. The compounds' ability to protect IMR-32 cells from $A\beta_{1-42}$ insult was investigated according to the published procedure.[32,33] To determine the cell viability, exponentially growing cells were plated at about 5000 cells per well 100 μL of fresh medium in 96-well tissue culture plates for 2 h. Cells were incubated with $A\beta_{1-42}$ (20 μM from a stock solution in DMSO) or Aβ plus 0.1 μM of each inhibitor for 48 h. The final DMSO concentration was less than 1%. After the incubation of cells in MTT solution (20 μL per well from 1 mg/mL stock solution) for 4 h at 37 °C. Cell lysis buffer (100 μL per well, 20% SDS/50% *N*,*N*-dimethylformamide, pH 4.7) was added, mixed, and

then colorimetric determination of MTT reduction was made at 570 nm using a microplate reader (Bio-Tek Instruments. Inc., Vermont, USA).

Acknowledgments

We thank Mr. Jeong-Ho Kang, Sangjae Lee, and Miss Hwa Jeong Lee for expert technical assistance and STC Life Science Co. Ltd for supporting instruments.

References and notes

1. Winkler, J.; Thal, L. J.; Gage, F. H.; Fisher, L. J. *J. Mol. Med.* **1998**, *76*, 555.
2. Lleo, A.; Greenberg, S. M.; Growdon, J. H. *Annu. Rev. Med.* **2006**, *57*, 513.
3. Carreiras, M. C.; Marco, J. L. *Curr. Pharm. Des.* **2004**, *10*, 3167.
4. Jacobsen, J. S.; Reinhart, P.; Pangalos, M. N. *Neuro. Rx.* **2005**, *2*, 612.
5. Mori, H. *Neuropathology* **2000**, *20*, 55.
6. Barril, X.; Orozco, M.; Luque, F. J. *Mini-Rev. Med. Chem.* **2001**, *1*, 255.
7. Kurz, A. *J. Neural. Transm. Suppl.* **1998**, *54*, 295.
8. Sugimoto, H. *Chem. Rec.* **2001**, *1*, 63.
9. Jann, M. W. *Pharmacotherapy* **2000**, *20*, 1.
10. Zarotsky, V.; Sramek, J. J.; Cutler, N. R. *Am. J. Health. Syst. Pharm.* **2003**, *60*, 446.
11. Gong, Y.; Chang, L.; Viola, K. L.; Lacor, P. N.; Lambert, M. P.; Finch, C. E.; Krafft, G. A.; Klein, W. L. *Proc. Natl. Acad. Sci. U.S.A.* **2003**, *100*, 10417.
12. Talaga, P. *Mini. Rev. Med. Chem.* **2001**, *1*, 175.
13. Mason, J. M.; Kokkoni, N.; Stott, K.; Doig, A. J. *Curr. Opin. Struct. Biol.* **2003**, *13*, 526.
14. Petkova, A. T.; Ishii, Y.; Balbach, J. J.; Antzutkin, O. N.; Leapman, R. D.; Delaglio, F.; Tycko, R. *Proc. Natl. Acad. Sci. U.S.A.* **2002**, *99*, 16742.
15. Luhrs, T.; Ritter, C.; Adrian, M.; Riek-Loher, D.; Bohrmann, B.; Dobeli, H.; Schubert, D.; Riek, R. *Proc. Natl. Acad. Sci. U.S.A.* **2005**, *102*, 17342.
16. Massi, F.; Straub, J. E. *J. Comput. Chem.* **2003**, *24*, 143.
17. Santini, S.; Mousseau, N.; Derreumaux, P. *J. Am. Chem. Soc.* **2004**, *126*, 11509.
18. Alvarez, A.; Opazo, C.; Alarcon, R.; Garrido, J.; Inestrosa, N. C. *J. Mol. Biol.* **1997**, *272*, 348.
19. De Ferrari, G. V.; Canales, M. A.; Shin, I.; Weiner, L. M.; Silman, I.; Inestrosa, N. C. *Biochemistry* **2001**, *40*, 10447.
20. Munoz, F. J.; Inestrosa, N. C. *FEBS Lett.* **1999**, *450*, 205.
21. Kwon, Y. E.; Kang, J. H.; Lee, H. J.; Lee, S. J. et al. PCT, 2003, WO 03/033489 A1.
22. Ellman, G. L.; Courtney, K. D.; Anders, V., Jr.; Feather-Stone, R. M. *Biochem. Pharmacol.* **1961**, *7*, 88.
23. Barril, X.; Kalko, S. G.; Orozco, M.; Luque, F. J. *Mini-Rev. Med. Chem.* **2002**, *2*, 27.
24. Greig, N. H.; Lahiri, D. K.; Sambamurti, K. *Int. Psychogeriatr.* **2002**, *14*, 77.
25. Ordentlich, A.; Barak, D.; Kronman, C.; Ariel, N.; Segall, Y.; Velan, B.; Shafferman, A. *J. Biol. Chem.* **1995**, *270*, 2082.
26. Lane, R. M.; Potkin, S. G.; Enz, A. *Int. J. Neuropsychopharmacol.* **2006**, *9*, 101.
27. Luo, W.; Yu, Q. S.; Kulkarni, S. S.; Parrish, D. A.; Holloway, H. W.; Tweedie, D.; Shafferman, A.; Lahiri, D. K.; Brossi, A.; Greig, N. H. *J. Med. Chem.* **2006**, *49*, 2174.
28. Kryger, G.; Silman, I.; Sussman, J. L. *Structure* **1999**, *7*, 297.
29. Colletier, J.; Fournier, D.; Greenblatt, H. M.; Stojan, J.; Sussman, J. L.; Zaccai, G.; Silman, I.; Weik, M. *EMBO J.* **2006**, *25*, 2746.
30. Munoz-Ruiz, P.; Rubio, L.; Garcia-Palomero, E.; Dorronsoro, I.; del Monte-Millan, M.; Valenzuela, R.; Usan, P.; Martinez, A., et al. *J. Med. Chem.* **2005**, *48*, 7223.
31. LeVine, H., 3rd *Protein Sci.* **1993**, *2*, 404.
32. Bartolini, M.; Bertucci, C.; Cavrini, V.; Andrisano, V. *Biochem. Pharmacol.* **2003**, *65*, 407.
33. Soto, C.; Kindy, M. S.; Baumann, M.; Frangione, B. *Biochem. Biophys. Res. Commun.* **1996**, *226*, 672.
34. Tjiernberg, L. O.; Lilliehook, C.; Callaway, D. J.; Naslund, J.; Hahne, S.; Thyberg, J.; Terenius, L.; Nordstedt, C. *J. Biol. Chem.* **1997**, *272*, 12601.
35. Findeis, M. A. *Biochim. Biophys. Acta* **2000**, *1502*, 76.
36. Piazzi, L.; Rampa, A.; Bisi, A.; Gobbi, S.; Belutti, F.; Cavalli, A., et al. *J. Med. Chem.* **2003**, *46*, 2279.
37. Kapkova, P.; Alptuzun, V.; Frey, P.; Erciyas, E.; Holzgrabe, U. *Bioorg. Med. Chem.* **2006**, *14*, 472.
38. Pollack, S. J.; Sadler, I. I.; Hawtin, S. R.; Tailor, V. J.; Shearman, M. S. *Neurosci. Lett.* **1995**, *197*, 211.
39. Jann, M. W. *Am. J. Health Syst. Pharm.* **1998**, *1*, S22.
40. Ezoulin, M. J.; Dong, C. Z.; Liu, Z.; Li, J.; Chen, H. Z.; Heymans, F.; Lelievre, L.; Ombetta, J. E.; Massicot, F. *Toxicol. In Vitro* **2006**, *20*, 824.
41. Peng, J. Z.; Remmei, R. P.; Sawchuk, R. J. *Drug Metab. Dispos.* **2004**, *32*, 805.